RESEARCH ARTICLE

Processes and characteristics of hydrogeochemical variations between unconfined and confined aquifer systems: a case study of the Nakdong River Basin in Busan City, Korea

Sang Yong Chung[1] · Rajesh Rajendran[2] · Venkatramanan Senapathi[3,4] · Selvam Sekar[5] · Paramasivam Chellamuthu Ranganathan[6] · Yun Yeong Oh[7] · Hussam Eldin Elzain[8]

Abstract

This study is to assess the hydrogeochemical characteristics of groundwater at the deltaic region of the Nakdong River Basin in the Busan Metropolitan City of Korea. The study area is covered by the Quaternary sedimentary deposits and the Cretaceous granites associated with unconformity. The thick sedimentary deposits consists of two aquifers, i.e., unconfined and confined aquifers on the basis of clay deposit. Groundwater samples were collected from seven boreholes: two from unconfined aquifer and five from confined aquifer systems during the wet season of 2017 year. ORP and DO indicates that the groundwater of the unconfined aquifer exists in the oxidization condition and that of the confined aquifer pertains in the reduction condition. Piper's trilinear diagram shows $CaSO_4$ type for groundwater of the unconfined aquifer, and NaCl type for that of the confined aquifer. Ionic concentrations of groundwater increase in the confined aquifer because of direct and reverse ion exchange processes. Carbonate weathering and evaporation are other mechanisms in the water-rock interaction. Saturation indices of dolomite and calcite are observed as oversaturated, while halite reveals undersaturation. Hierarchical cluster analysis (HCA) exhibits that cluster 1 and cluster 2 represents the properties of groundwater in unconfined and confined aquifers, respectively. Factor analysis shows that groundwater of the confined aquifer is much influenced by seawater, and includes heavy metals of iron and aluminum. Groundwater samples in unconfined and confined aquifers are located at the rock weathering and evaporation zones in the Gibbs diagram. Inverse geochemical modeling of PHREEQC code suggests that carbonate dissolution and ion exchange of major ions are the prevailing geochemical processes. This comprehensive research provides the distinguished hydrogeochemical characteristics of groundwater in confined and unconfined aquifer systems of the Nakdong River Basin in Busan City, Korea.

Keywords Hydrogeochemical analysis · Geostatistical analysis · Inverse geochemical modeling · Unconfined aquifer · Confined aquifer · Nakdong River basin

Responsible editor: Philippe Garrigues

✉ Venkatramanan Senapathi
  venkatramanan@tdtu.edu.vn

1   Department of Earth and Environmental Sciences, Institute of Environmental Sciences, Pukyong National University, Busan 48513, South Korea

2   Department of Civil Engineering, Indian Institute of Science, Bangalore, India

3   Department for Management of Science and Technology Development, Ton Duc Thang University, Ho Chi Minh City, Vietnam

4   Faculty of Applied Sciences, Ton Duc Thang University, Ho Chi Minh City, Vietnam

5   Department of Geology, V. O. Chidambaram College, Tuticorin 628 008, India

6   Department of Remote Sensing, Bharathidasan University, Tiruchirappalli 620024, India

7   Department of Earth & Environmental Sciences, Korea-CO2 Storage Environmental Management (K-COSEM) Research Center, Korea University, Seoul 02841, South Korea

8   Department of Earth & Environmental Sciences, Division of Earth Environmental System Science, Pukyong National University, Busan 48513, South Korea

Introduction

Hydrogeochemical processes in aquifer materials have an intensive effect on groundwater quality. The identification of hydrogeochemical processes renders the comprehension for the origin of water quality due to the interaction with aquifer materials. Hydrogeochemical processes such as dissolution, mixing, evaporation, and ion exchange control the concentrations of ions in groundwater (Rajesh et al. 2012). The geochemical characteristics of groundwater are also influenced by the chemical components of recharge water as well as geological processes in the subsurface. Hydrogeochemical processes support the ideas for the influences of water/rock interaction and anthropogenic impacts on groundwater quality (Kumar et al. 2009; Li 2016; Wu and Sun 2016). Statistical techniques and inverse geochemical modeling are noteworthy methods to study the hydrogeochemical variations (Belkhiri et al. 2010). It is useful for the hydrogeochemical study to determine the parameters of groundwater mixing in different aquifers (Razack and Dazy 1990), to describe the control of hydrogeochemical processes (Adams et al. 2001), and to separate anthropogenic impacts from the background (Pereira et al. 2003). Hierarchical cluster analysis (HCA) is also useful for geochemical model development and source identification (Meng and Maynard 2001). The Gibbs diagram and correlation analysis are important to study the sources of different ions in groundwater chemistry (Wu et al. 2014; Li et al. 2010). Parkhurst and Appelo (1999) used a geochemical mole-balance model in the inverse geochemical modeling of PHREEQC and calculated the phase mole transfers to interpret the changes in a primary and an ending water constituent along the flow direction in an aquifer system.

Generally, the deltaic aquifer is the key source of water necessary for human living and agricultural activities all over the world. A number of factors including natural processes and anthropogenic activities affect the groundwater quality (Helena et al. 2000; Stark et al. 2000; Mohamed and Elmahdy 2015; Zaki et al. 2019). Dissolvable chemical components of groundwater are reliant on the time of interaction between water and rock bearing sediments, and microbiological constituents are influenced by urban, industrial, and agricultural activities (Daniele et al. 2013). The identification of the processes to affect the groundwater quality is crucial to achieve the control and enhancement of water quality in the future. It is reported that the inverse geochemical modeling is an important method to realize the groundwater evolution by various authors (Sun 1994; McLaughlin and Townley 1996; Thilagavathi et al. 2019). Various techniques have been used for groundwater quality assessment.

Combined methods of statistical methods, geospatial techniques, and geochemical modeling were used in this study. These methods can elucidate the formation of various groundwater quality (de Caritat et al. 2019; Brindha et al. 2017).

Several researchers have been interested in geological features, sea level change, and the geochemistry of river water and groundwater in the study area. Yoo et al. (2014a) studied the evolution of inner shelf deposits with sediments supplies in response to the late Quaternary sea level changes. Yoo et al. (2014b) showed that most of deltaic sediments were deposited in the study area since the last Glacier Period of the late Pleistocene. The previous study conducted by Chung et al. (2014, 2016, 2019) evaluated the hydrogeochemical characteristics of the Nakdong River water and sediments, using geochemical and geostatistical methods. Venkatramanan et al. (2014, 2017) showed that the geochemical processes of surface water and adjacent deltaic groundwater near the study area were related with weathering and ion exchange, using saturation index (SI). The previous research mainly focused on the qualities of surface water, groundwater, and sediment in the Nakdong River Basin.

However, we have not carried out the combined studies of paleo-geological approach, hydrogeochemical analysis, geostatistical analysis, and inverse geochemical modeling to identify the overall hydrogeochemical processes of groundwater in the thick sedimentary deposits of the study area. This study is the first comprehensive research to reveal the hydrogeochemical processes and the groundwater characteristics of unconfined and confined aquifers in the Nakdong River Basin. It will be useful for the management and conservation of groundwater in this region.

Study area

The Nakdong River including eight tributaries is the largest river in South Korea (Fig. 1). Its length is 525 km and the total watershed area is 24,000 km^2. The study area is located at a part of the Nakdong River basin in Busan Metropolitan City of Korea. The annual average temperature and the precipitation (2008–2017 year) range from 14.5 to 15.7 °C, and from 1014.4 to 1983.3 mm (Fig. 2), and their average values are 15.09 °C and 1484.0 mm, respectively. The relation between temperature and precipitation was proportional from 2008 to 2010, and from 2015 to 2017. On the other hand, their relation was changed to the inverse proportion from 2011 to 2014. Greenhouses cultivating fruits and vegetables are popular at the western part of the study area. Large commercial and small industrial facilities exist at the eastern part of the study area.

The basement below deltaic sediments is the Cretaceous granitic rock, and the sediments uncomfortably overlay the basement. Groundwater quality in the sediments was influenced by chemical components of sediments as well as seawater. Many studies have been concentrated on the geochemical processes of river water, the late Quaternary sea level changes, and the geological relation between deltaic sediments and the basement. The main channel is represented by

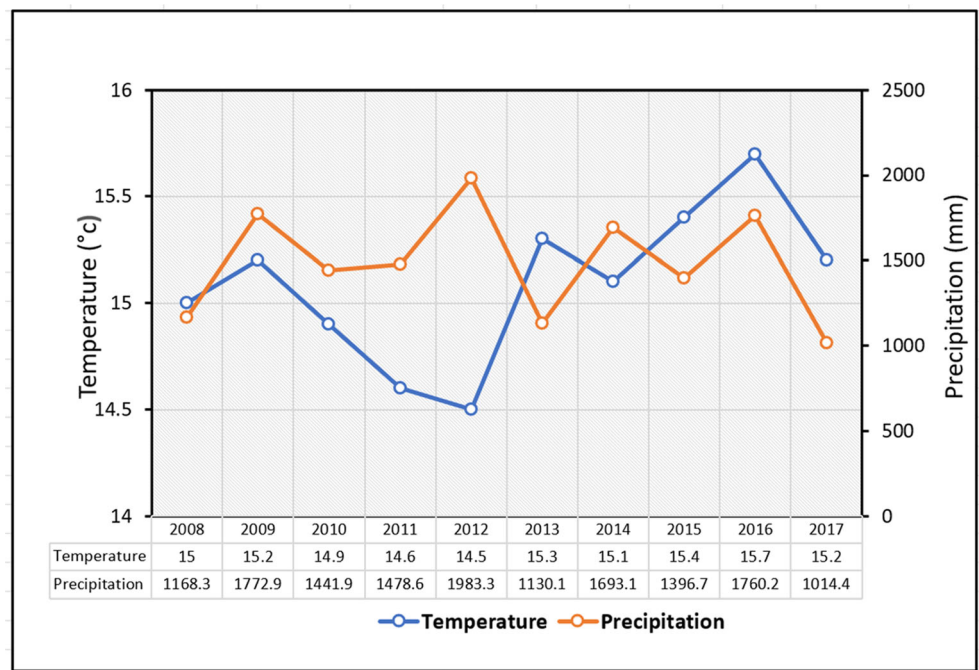**Fig. 1** Study area with groundwater sampling wells (Source: Google earth)
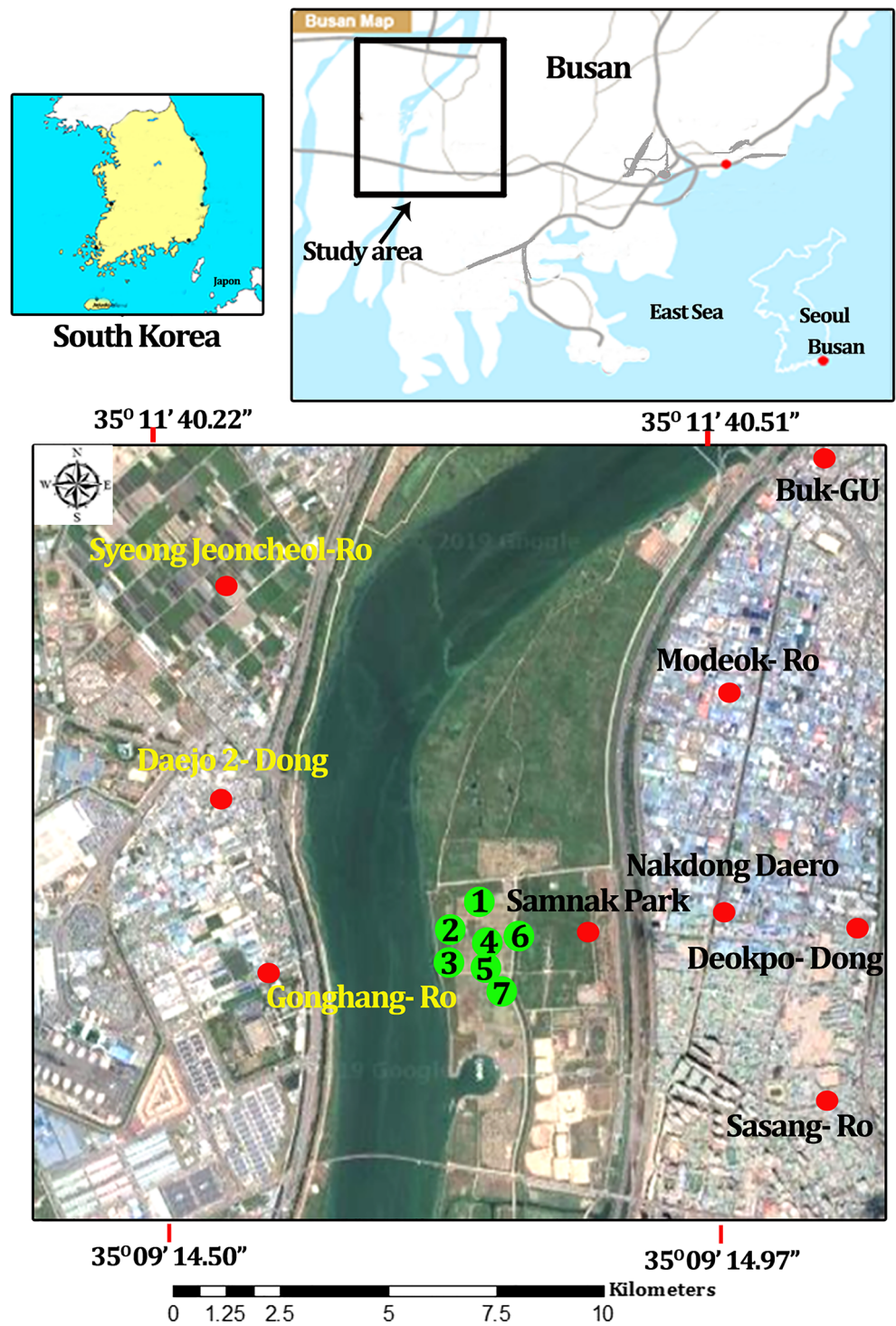
a longitudinal drainage pattern parallel to the main fault and the minor channels are connected to the main channel to proceed to a dendritic drainage pattern. The Cretaceous basement rocks of biotite granite and hornblende granodiorite are uncomfortably overlain by Quaternary formations (Fig. 3). The elevation of the study area ranges from 1 to 2 m above the mean sea level (Fig. 4). The center and the southeastern part of the area are a higher than the other areas. Evaporite and

Fig. 2 Temperature and precipitation from 2008 to 2017 year in Busan Metropolitan City, Korea

	2008	2009	2010	2011	2012	2013	2014	2015	2016	2017
Temperature	15	15.2	14.9	14.6	14.5	15.3	15.1	15.4	15.7	15.2
Precipitation	1168.3	1772.9	1441.9	1478.6	1983.3	1130.1	1693.1	1396.7	1760.2	1014.4

—○— **Temperature** —○— **Precipitation**

gypsum deposits are present in the lower basin of the Nakdong River. The Quaternary sedimentary deposits are present in the sequence of upper clayey sand layer, clay layer, lower sand layer, and gravel layer in sequence, and were formed by the rise of sea level after the last Glacier Epoch during the Quaternary Period (Yoo et al. 2014a; Yoo et al. 2014b). The clay layer is about 15 m thickness as an impermeable confining layer and divides the sedimentary deposits into two aquifers, i.e., unconfined aquifer and confined aquifer.

Based on these hydrogeological sections of Fig. 5, OW-1, OW-2, OW-5, OW-6, and OW-7 of confined aquifers are
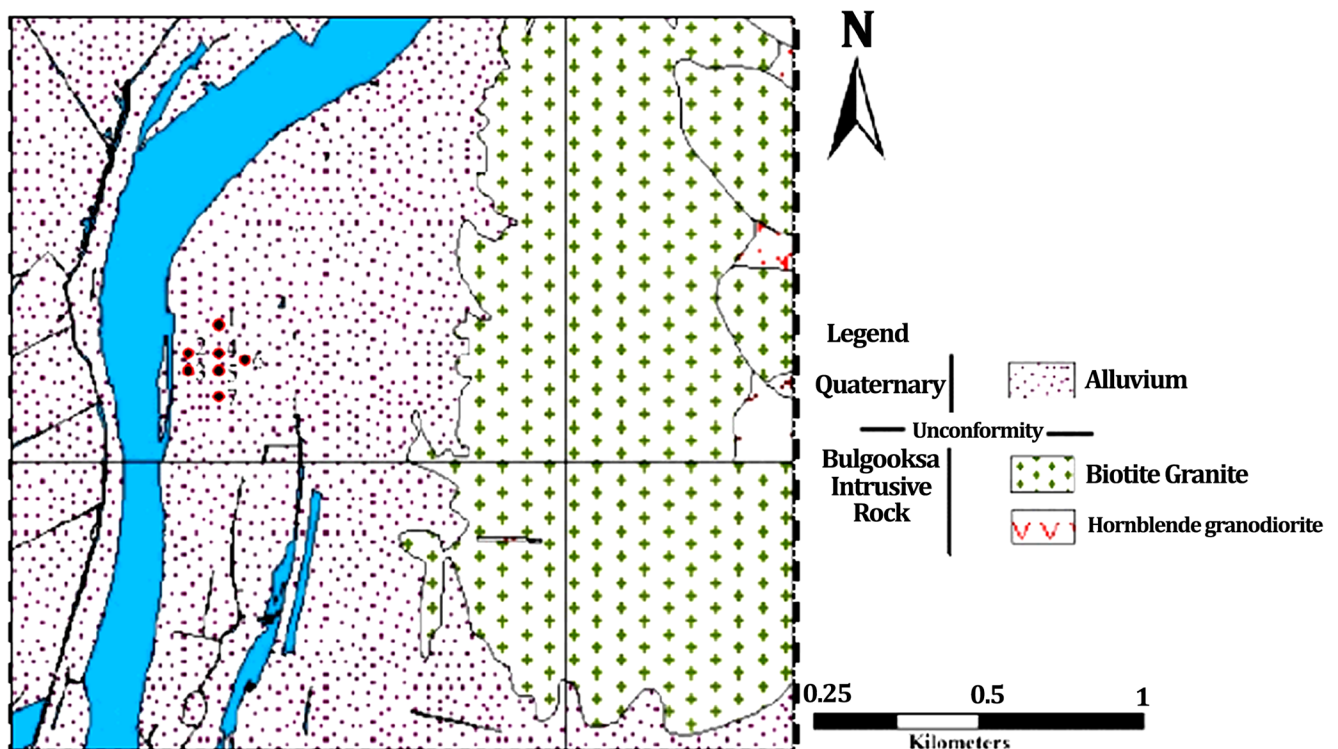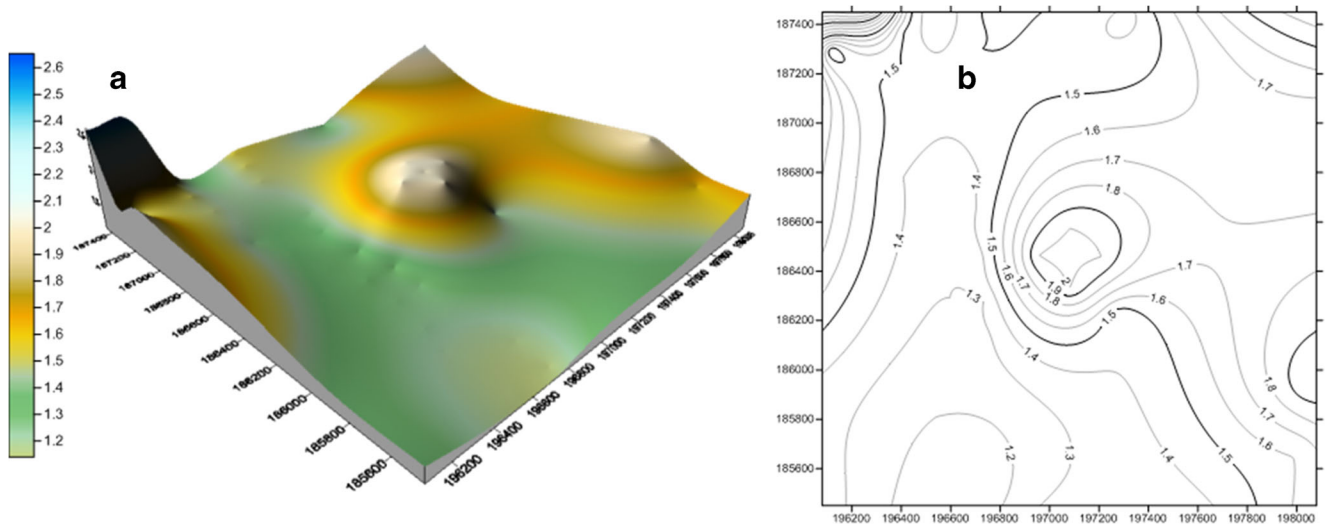

Fig. 3 Geology of the Nakdong deltaic region

Fig. 4 Topography of the study area (**a**) 3D surface (**b**) contour map

composed of seven distinct layers of landfill (0.6 to 1 m in thickness), upper sand (6 to 12 m), clay (10 to 21 m), lower sand (31 to 36 m), gravel (2.2 to 11 m), weathered rock (1.5 to 12 m), and bedrock (< 10 m). OW-3 and OW-4 of unconfined aquifers consist of landfill and upper sand. The clay layer is a boundary between the unconfined aquifer and confined aquifer. Porosity

and hydraulic conductivity of sediment layers are from 37 to 59% and from 1.7 to 300 m/day, respectively. Groundwater level ranges from − 1.4 to 1.1 m above the mean sea level. The groundwater flow shows several directions, i.e., from the north to the south and from the east to the west in the upper part region, and from the center to the southwest and from the center to the
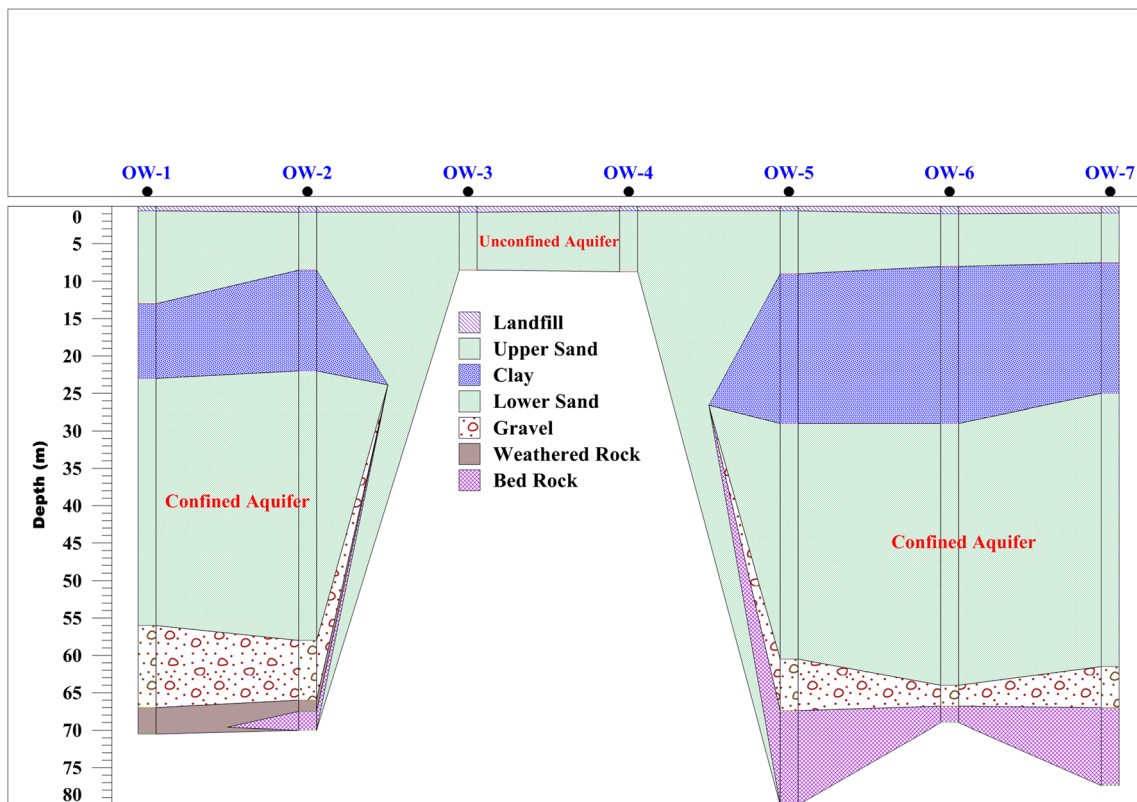

Fig. 5 Hydrogeological cross-section of boreholes in Nakdong deltaic region
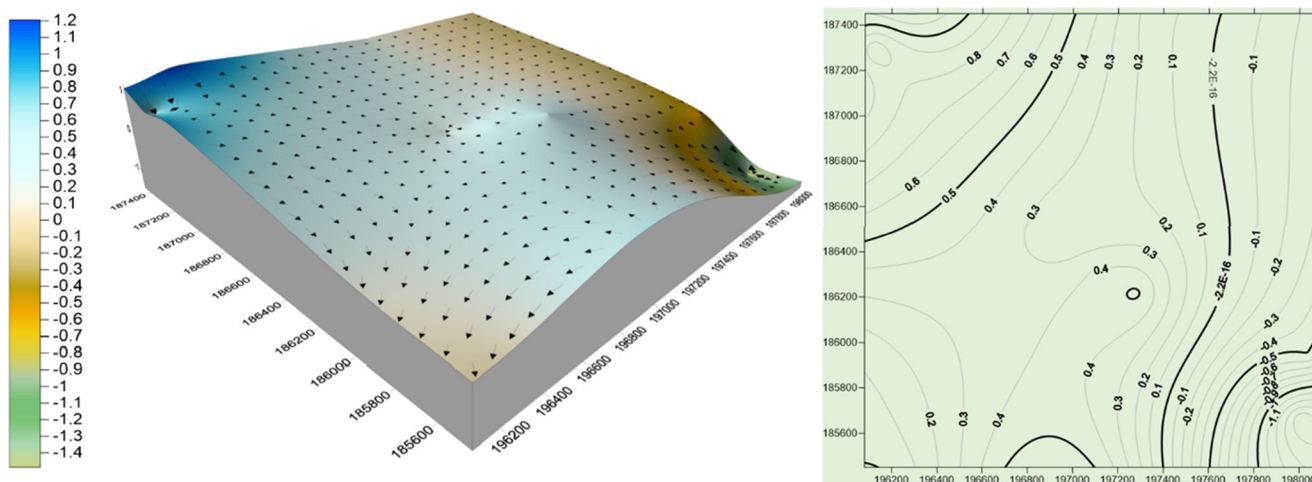
Fig. 6 Groundwater flow diagram and contour map of piezometric surface (m, msl)

southeast in the lower part region (Fig. 6). The water level of the northwestern part is higher, and that of the southeastern part is lower than the other areas.

Materials and methods

Groundwater sampling and analysis

Groundwater samples were collected at seven boreholes in the wet season of the year 2017. The sampling, preservation, and transportation of groundwater samples followed the standard methods of the American Public Health Association (APHA 1995). The sampling bottles were soaked in 1:1 diluted HCl solution for 24 h before sampling and then washed with distilled water. pH, electrical conductivity (EC), total dissolved solids (TDS), dissolved oxygen (DO), and oxidation-reduction potential (ORP) were measured in the field, using a portable water quality meter (Horiba U-51, Japan). Major elements (Na, Ca, Mg, K, Cl, SO_4) and trace elements (Si, Al, Mn, Fe, As) were analyzed by using an atomic absorption spectrometer (AAS Graphite Furnace (GF), PerkinElmer 400) and ion chromatography (IC, Water 431). Detection limits of IC calculated were 0.05–0.58 mg/L for the anions and 0.05–0.38 mg/L for the cations, whereas repeatability values were below 2.26, 2.76, and 2.90% for peak height, peak area, and retention time, respectively. AAS represents the detection limits of elements such as Al (0.1 mg/l), Si (1.0 mg/l), Fe (0.06 mg/l), Mn (0.05 mg/l), and As (0.01 mg/l). The concentrations of CO_3 and HCO_3 were determined by the titration method. Standards and blanks were run regularly to check accuracy (QA/QC) of the procedures. The accuracy of chemical analysis was established by computing ion-balance errors within ±5%.

Geostatistical analysis

The STATISTICA version 13 (StatSoft, 2015) software was used for the multivariate geostatistical analysis such as the hierarchical cluster analysis (HCA). HCA categorizes groundwater samples into the real groups assembled on the aligned Euclidean distance between the distinct hydrogeochemical variables. Data was calculated by Q-mode in order to acquire the comparison of data between cases. The correspondence coefficient was used in the simple distance demarcated in the Euclidean space (Ashley and Lloyd 1978), and the clustering was made by the Ward's linkage technique. Factor analysis (FA) reveals only suitable components among many hydrogeochemical data and reduces many data to a limited number of variables called factors (Adams et al. 2001; Ashley and Lloyd 1978; Hussein 2004). Seventeen components of pH, EC, TDS, ORP, DO, Na, K, Ca, Mg, Cl, HCO_3, SO_4, SiO_2 Fe, Mn, As, and Al were utilized for the geostatistical analyses.

Inverse geochemical modeling

The conventional conditions are required in the application of the inverse geochemical modeling: (1) initial and final groundwater samples must flow along the same flow direction, (2) dispersion and diffusion do not considerably affect groundwater chemistry, (3) chemically steady-state condition should be attained in the groundwater aquifer matrix during the time considered, and (4) mineral phases used in the inverse calculation are or were present in the aquifer (Zhu and Anderson 2002). The inverse geochemical modeling of PHREEQC was used to examine the geochemical processes of groundwater. PHREEQC provides the opportunity for computing the mass equilibrium along a particular flow path regarding the effects of groundwater quality. Inverse modeling is used to evaluate the moles of minerals and gases dissolved or precipitated to understand the variance in composition

between initial and final water end members (Parkhurst and Appelo 1999).

Inverse modeling using PHREEQC of water is saturated or supersaturated with respect to the mineral. If IAP is less than KT, the solution is undersaturated with respect to the mineral, Now, this indices log (IAP/KT) was calculated to know if: SI = log (IAP/KT) = 0; equilibrium state, SI = log (IAP/KT) < 0; undersaturation state in mineral dissolution condition, while SI = log (IAP/KT) > 0; oversaturation state in mineral precipitation condition (Chidambaram et al. 2012).

It can be applied to derive geochemical reactions for the difference in chemical composition of groundwater along a flow path. Both aqueous speciation and saturation indices are also calculated by the code. The flow paths of the study area are chosen according to the various hydrogeological characteristics. The mole transfer results are reported as mol/kg of water. The positive values of mass transfer suggest the dissolution of minerals and the negative values exhibits precipitation.

Results and discussion

Groundwater chemistry

The statistical analysis of chemical constituents of the groundwater samples is shown in Table 1. pH values range 7.16 to 7.76 and represent a slightly alkaline property in both unconfined and confined aquifers. Electrical conductivity (EC) values range from

40,660 to 41,550 μS/cm in the confined aquifer, and from 1290 to 2030 μS/cm in the unconfined aquifer.

The low EC in the unconfined aquifer is influenced by precipitation and the Nakdong River water. The groundwater of the unconfined aquifer is interacted with the Nakdong River water which is a normal fresh water protected by a big barrage installed at the end of the river. On the other hand, the high EC in the confined aquifer is mainly due to the impact of seawater (Chung et al. 2016). Total dissolved solids (TDS) vary from 840 to 1320 mg/l in the unconfined aquifer and from 26,430 to 29,980 mg/l in the confined aquifer. Higher values of EC and TDS were observed from the wells OW-1, OW-2, OW-5, OW-6, and OW-7 in the confined aquifer. Groundwater in the unconfined aquifer is a little contaminated by the contaminants derived from the ground surface such as industrial and domestic effluents or fertilizers (Chung et al. 2016). However, groundwater in the confined aquifer is a seawater induced from the sea due to the sea level rise after the last Glaciation of the Pleistocene Epoch (Lee et al. 2008).

Oxidation reduction potential (ORP) ranges from − 12.20 to 81.40 mV in the unconfined aquifer, and from − 171.50 to − 86.70 mV in the confined aquifer. Dissolve oxygen (DO) ranges from 3.54 to 4.24 mg/l in the unconfined aquifer, and from 0.86 to 3.15 mg/l in the confined aquifer. Figure 7a showed that there is a good correlation between DO and ORP because groundwater of the confined aquifer and unconfined aquifer is in the reduction and oxidation conditions, respectively. The state of Low DO and high ORP is in the confined aquifer and the state of high DO and low ORP is in the

Table 1 Statistical summary of hydrogeochemical components of groundwater

Variable	Unit	Unconfined aquifer				Confined aquifer			
		Minimum	Maximum	Mean	SD	Minimum	Maximum	Mean	SD
EC	μS/cm	1290.00	2030.00	1660.00	523.26	40,660.00	41,550.00	41,144.00	320.52
TDS	mg/L	840.00	1320.00	1080.00	339.41	26,430.00	29,980.00	27,330.00	1487.88
pH		7.45	7.76	7.61	0.22	7.16	7.68	7.40	0.23
ORP	mV	− 12.20	81.40	34.60	66.19	− 171.50	− 86.70	− 125.32	32.51
DO	mg/L	0.86	3.15	1.66	1.40	3.54	4.24	3.89	1.57
Na	mg/L	58.40	180.58	119.49	86.40	8402.87	9007.27	8648.30	220.76
Ca	mg/L	128.79	240.48	184.63	78.98	338.35	474.84	413.55	49.38
Mg	mg/L	50.61	72.30	61.45	15.34	970.98	1031.38	1001.30	27.47
K	mg/L	8.60	8.90	8.75	0.21	281.37	303.50	292.91	9.91
Cl	mg/L	181.82	189.72	185.77	5.59	17,107.34	17,898.17	17,533.39	290.84
SO$_4$	mg/L	284.92	664.68	474.80	268.53	8.46	63.70	32.67	22.35
HCO$_3$	mg/L	434.63	462.38	448.50	19.63	1732.40	1915.40	1817.80	85.40
SiO$_2$	mg/L	9.72	10.35	10.04	0.45	6.47	7.40	7.06	0.36
Al	mg/L	0.07	0.08	0.08	0.01	0.08	0.22	0.12	0.06
Mn	mg/L	0.70	3.63	2.16	2.07	1.28	1.66	1.51	0.15
As	mg/L	BDL	0.06	0.03	0.04	0.10	0.24	0.15	0.06
Fe	mg/L	0.2	1.77	0.96	1.14	4.41	11.62	7.01	2.96
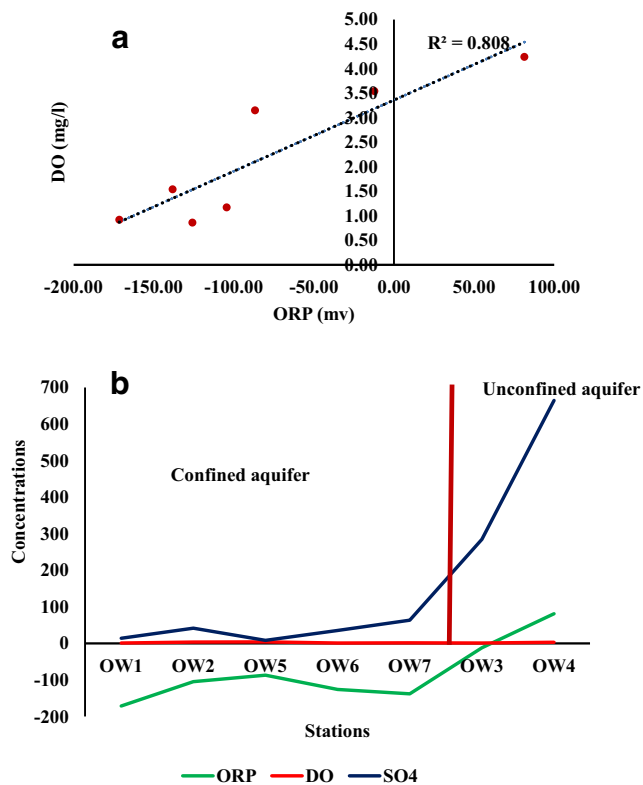
Fig. 7 Relationship between the **a** ORP vs. DO and **b** ORP, DO, and SO4

the confined aquifer is in the reduced environment (Chung et al. 2018). The lower ORP value increases Mn concentration by the dissolution of manganese oxides. The increase of Fe concentration with decreasing ORP is influenced by the reductive dissolution of iron oxyhydroxides (Bose and Sharma 2002). Concentration of DO plays a vital role in supporting aquatic life in running water and is vulnerable to slight environmental changes (Iticescu et al. 2013).

Groundwater samples of the confined aquifer represented that the dominant ions were Na, Mg, Ca, and K in cations and Cl, HCO3, and SO4 in anions. Na, Mg, K, Cl, and SO4 were influenced by paleo-seawater transgressed from the Quaternary Period (Yoo et al. 2014b). Many shell fragments were deposited in the confined aquifer during the transgression of seawater. Ca and HCO3 were derived mainly from the shell fragments. Ca could be also produced by the interaction between sediments (feldspar and mafic minerals) and water, and HCO3 could come from the precipitation. However, they did not have large quantities. In the unconfined aquifer, Ca, Na, and Mg were dominant in cations, and HCO3, SO4, and Cl were abundant in anions. Ca and HCO3 were major components in the unconfined aquifer, and they were representative ions for most of the groundwater in Korea. The variation of major ionic chemistry was controlled by rainfall, domestic and industrial effluents, or fertilizer (Venkatramanan et al. 2017; Chung et al. 2019).

Hydrogeochemical processes and ion exchange

The chemical data of groundwater samples were plotted in the Gibbs diagram (Fig. 8). Groundwater samples of the

unconfined aquifer. Figure 7b represented the variation of ORP, DO, and SO4, and the concentration of SO4 increased in the oxidation condition. It suggested that SO4 derived from the anthropogenic sources. ORP indicates that groundwater of the unconfined aquifer is in the oxidized environment, but that of

Fig. 8 Gibbs diagrams showing the mechanism controlling groundwater chemistry of **a** TDS vs. cations and **b** TDS vs. anions
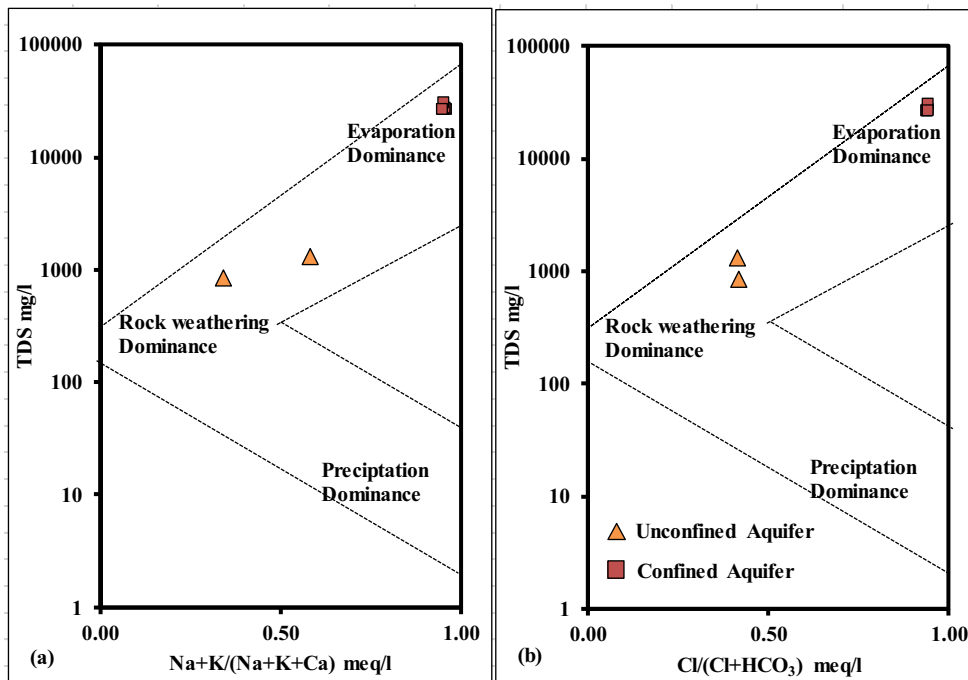
unconfined aquifer were influenced by the chemical weathering with dissolution of rock forming minerals, and groundwater samples of confined groundwater were plotted in the evaporation zone. The groundwater of NaCl type in the confined aquifer was saline quality because this formation was affected by marine transgression and regression in the Quaternary Period (Ferguson and Gleeson, 2012, Cho et al. 2017).

Chemical components of groundwater were used to identify the hydrogeochemical processes and mechanisms in aquifer materials. In the $(Ca^{2+} + Mg^{2+})$ versus $(HCO_3^- + CO_3^{2-})$ diagram

(Fig. 9a), all samples of unconfined and confined aquifers fall above the equiline 1:1. It suggests that a large amount of Ca^{2+} and Mg^{2+} is resulted from carbonate sources (Rajib Paul et al. 2019). In the $(Ca^{2+} + Mg^{2+})$ versus TC (Total cation) diagram (Fig. 9b), all samples of unconfined and confined aquifers fall below the equiline 1:1. It represents that Ca and Na are major components of cations in the unconfined aquifer, and that Ca is not the major component of cations in the confined aquifer.

In the plot of $(Na^+ + K^+)$ versus TC (total cation) (Fig. 9c), all samples of unconfined and confined aquifers fall below the

Fig. 9 Relationships between major ions and their ionic exchange processes: **a** Ca + Mg vs. HCO3 + CO3, **b** Ca + Mg vs. TC, **c** Na + K vs. TC, **d** SO4+ Cl vs. Na + K, **e** (Ca + Mg) − (HCO3 + SO4) vs. Na-Cl, **f** Ca + Mg vs. HCO3 + SO4, and **g** Ca + Mg vs. C
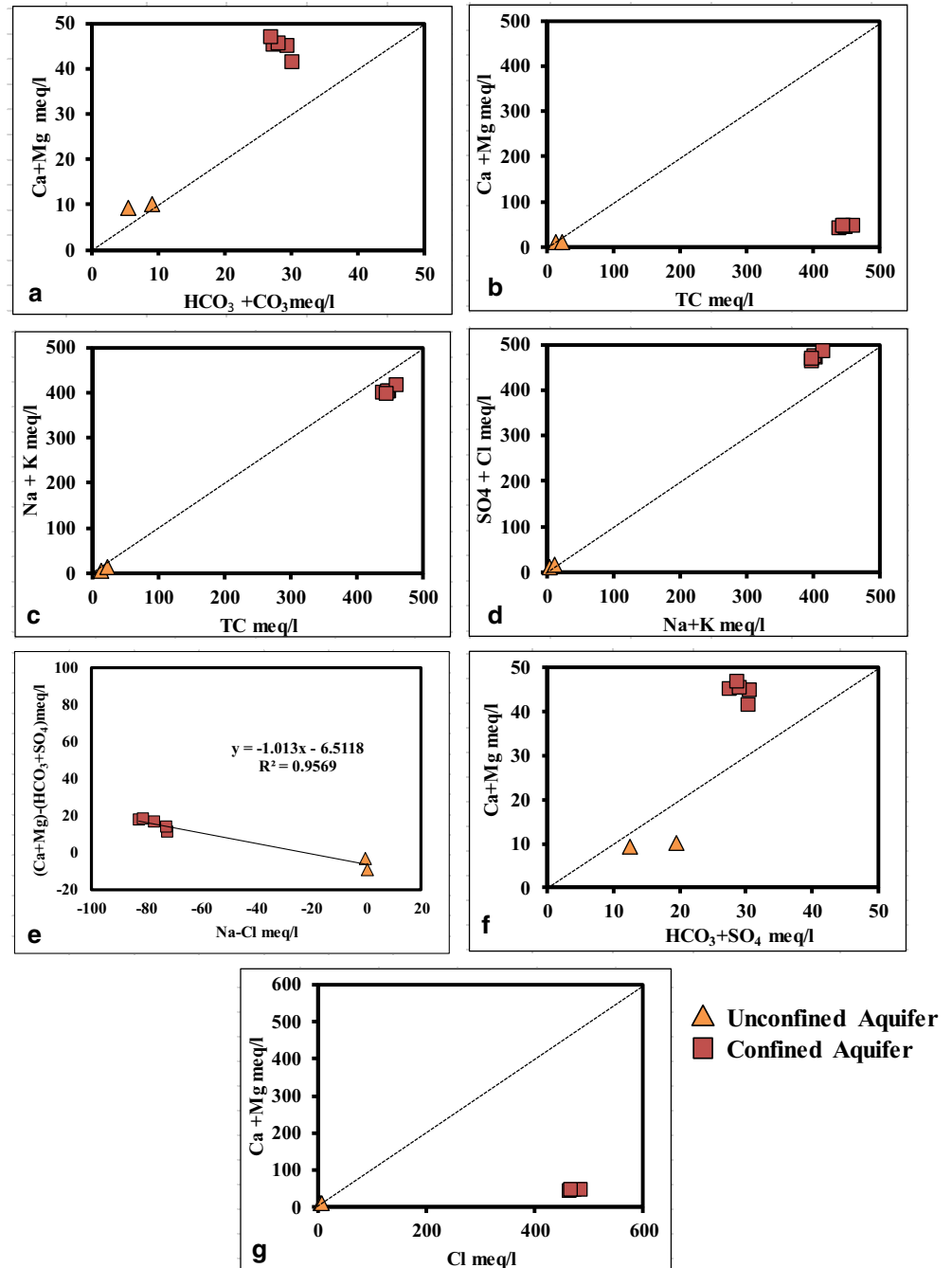
equiline 1:1. It shows that Na and K are all major components of cations in unconfined and confined aquifers. In the plot of $(SO_4^{-2} + Cl^-)$ versus $(Na + K)$ (Fig. 9d), the samples of the unconfined aquifer fall on the equiline and the samples of the confined aquifer fall above the equiline. It indicates that the quantity of $(SO_4^{-2} + Cl^-)$ are proportional to the quantity of $(Na + K)$ in all samples of unconfined and confined aquifers. The ratio of $(Ca^{2+} + Mg^{2+} - HCO_3^- + SO_4^2)$ versus (Na^+-Cl^-) was used to evaluate the direct and reverse ion exchange processes of groundwater samples (Fig. 9e). In this plot, unconfined and confined aquifer samples follow a straight line $(R^2 = 0.95)$ with a slope of -1.01, and it suggests a reverse ion exchange (Post and Abarca, 2009).

In the plot of $(Ca^{2+} + Mg^{2+})$ versus $(HCO_3^- + SO_4^{2-})$ (Fig. 9f), the samples of unconfined and confined aquifers are close to the equiline of 1:1, and it represents that carbonate minerals are dominant in the aquifer matrix. Direct ion exchange tends to move the samples to the right side in excess of $(SO_4^{2-} + HCO_3^-)$ (Datta and Tyagi 1996). In case that a reverse ion exchange process is dominant, samples shift to the left due to a large excess of $(Ca^{2+} + Mg^{2+})$. In the study area, unconfined aquifer and confined aquifer samples exhibit the direct and reverse ion exchange processes, respectively. The plot of $(Ca^{2+} + Mg^{2+})$ versus Cl^- (Fig. 9g) shows that they have a good relation in unconfined aquifer and do not have a relation in the confined aquifer because chloride of the confined aquifer was originated mainly from seawater (Werner et al. 2013).

Evaporation processes

In general, the evaporation process would cause an increase in concentration of all mineral species in water. In case that evaporation process is dominant under no precipitation of mineral species, the ratio of (Na^+/Cl^-) is not altered (Jankowski and Acworth 1997). The plot of EC versus (Na^+/Cl^-) would give a horizontal line under the normal evaporation. If the (Na^+/Cl^-) ratio is nearly equal to 1.0, sodium is derived from a halite solution. If the ratio is greater than 1.0, sodium is normally released from a silicate

weathering (Mayback 1987). The (Na^+/Cl^-) ratio of the study area ranges from 0.82 to 1.02 (Fig. 10a). The samples of the confined aquifer fall below the ration of 1.0, and the sodium in the confined aquifer may come from the dissolution of halite. A sample of the unconfined aquifer fall above the ratio of 1.0, and the sodium may be derived from a silicate weathering (Prasanna et al. 2019). The $(Na+/Cl^-)$ versus EC diagram exhibits an inclined trend line, and evaporation may not be the major hydrogeochemical processes for groundwater quality. The plot of Na^+ versus Cl^- (Fig. 10b) represents that the samples of the unconfined aquifer fall near the equiline showing the nearly equal concentration of Na^+ and Cl^-. The samples of the confined aquifer display below the equiline, indicating the smaller concentration of Na^+ than Cl^-. This phenomenon can be due to a halite solution and other related minerals in evaporate deposits (Walker et al. 1991).

Carbonate dissolution

The ratio of calcium and magnesium is useful for understanding the carbonate dissolution in groundwater. In case of the ratio is 1.0, groundwater is controlled by dolomite dissolution. The ratio of 1–2 indicates calcite dissolution (Maya and Louks 1995). The ratio over 2.0 suggests the silicate minerals dissolution (Rajesh et al. 2012). The ratio of the unconfined aquifer ranges from 4.09 to 5.35, and it indicates the result of silicate minerals dissolution (Fig. 11). The ratio of the confined aquifer is 0.53 to 0.78, and it is less than the line 1.0. The carbonate of the confined aquifer might be the result of dolomite dissolution. The confined aquifer of the study area contains many shell fragments in sediments during the deposition and paleoseawater transgressed from the Quaternary Period (Yoo et al. 2014b). This process is liable for high concentrations of Ca^{2+}, Mg^{2+}, and HCO_3^- in groundwater. Availability of carbonate minerals in the recharge area and silicate weathering are the major causes which lead to the increase in CO_3^{2-} and HCO_3^- concentration in groundwater (Appelo and Postma 2005; Brindha et al. 2017).
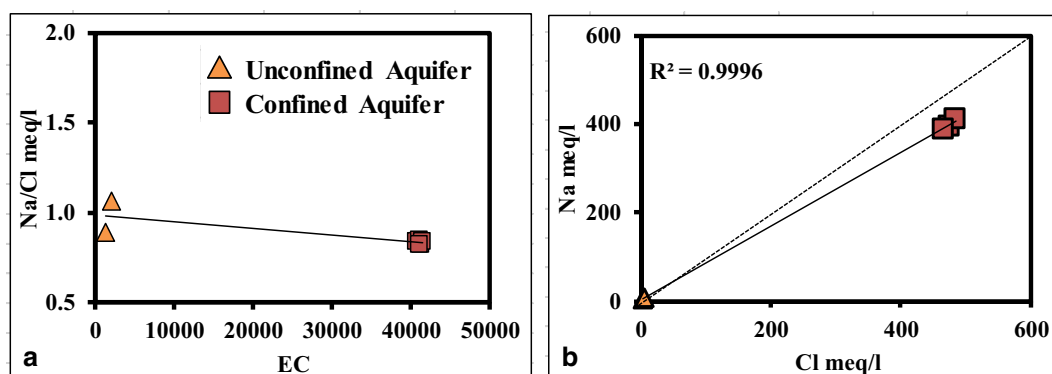

Fig. 10 Relationship between evaporation processes **a** Na^+/Cl^- vs. EC, **b** Na^+ vs. Cl^- in confined and unconfined aquifer systems
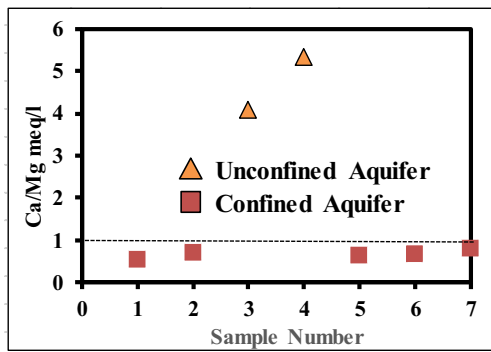
Fig. 11 Relationship between carbonate dissolution of Ca^{2+}/Mg^{2+} vs. Sample number in confined and unconfined aquifer system

Hydrogeochemical facies

Hydrogeochemical facies can be used to infer the effects of chemical reactions in the water-rock interaction. The graphical form of the Piper diagram was applied to identify the dominant groundwater types in this study (Fig. 12). This plot exhibits useful properties and relationships for large sample groups (Srivastava and Ramanathan 2008). Accordingly, two major groundwater types were dominant in this region: Ca $(HCO_3)^2$ and $CaSO_4$ for the unconfined aquifer and NaCl for the confined aquifer. The diagram suggests that the groundwater of the unconfined aquifer was contaminated by domestic and industrial wastes. While, the groundwater of the confined aquifer suggested that the NaCl type was derived from the seawater incursion of sea level rise since the late Pleistocene Epoch (Cho et al. 2017).
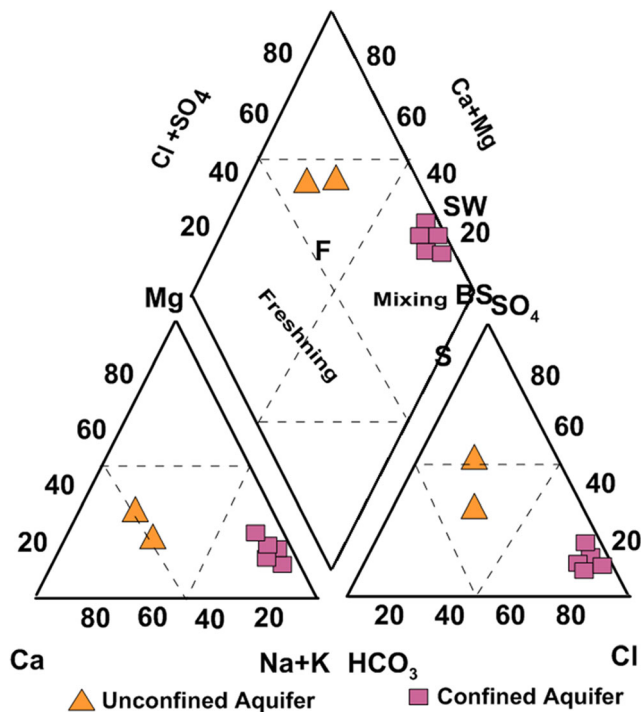

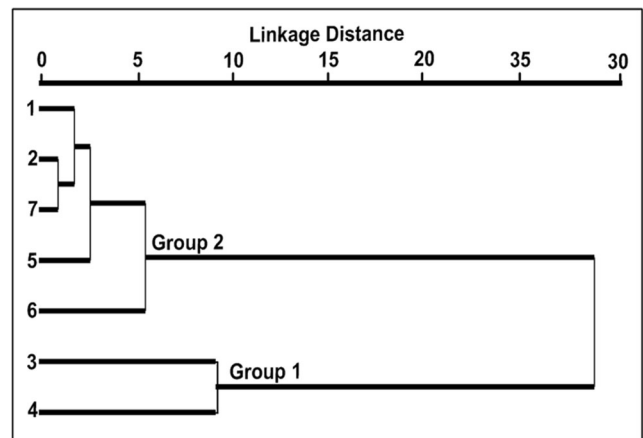**Fig. 12** Piper diagram for hydrogeochemical facies of groundwater samples

Fig. 13 Dendrogram of the Q-mode hierarchical cluster analysis

Multivariate statistical analysis

Hierarchical cluster analysis

The hierarchical cluster analysis was carried out for seven7 groundwater samples with the components of pH, EC, TDS, DO, ORP, Ca^{2+}, Mg^{2+}, Na^+, K^+, Cl^-, SO_4^{2-}, HCO_3^-, SiO_2, Al, Fe, Mn, and As. Two primary groups were determined on graphical interpretation of the dendrogram (Fig. 13). Group 1 includes well nos. 3 and 4 representing unconfined aquifer samples. Group 1 contains the $CaSO_4$ types of groundwater with lower TDS and EC than Group 2. Group 2 comprises of well nos. 1, 2, 5, 6, and 7 with confined aquifer samples. The

Table 2 Factor loadings of Factor 1 and Factor 2 (italic text represents significant factor)

Variables	Factor 1	Factor 2
EC	*0.99*	0.09
TDS	*0.99*	0.13
pH	− 0.35	*− 0.87*
ORP	*− 0.94*	0.28
DO	− 0.09	*0.58*
Na	*0.99*	0.10
Ca	*0.88*	0.25
Mg	*0.99*	0.10
K	*0.99*	0.11
Cl	*0.99*	0.10
SO$_4$	*− 0.91*	0.07
HCO$_3$	*0.99*	0.04
Fe	0.18	*− 0.82*
Mn	0.21	0.27
As	*0.79*	− 0.50
Si	*− 0.98*	− 0.14
Al	0.42	*0.67*
Eigenvalue	11.39	2.71
% variance	66.99	15.94
Cumulative %	66.99	82.93
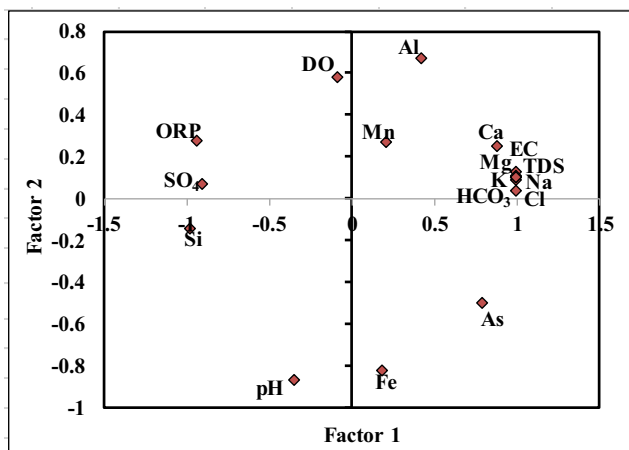
Fig. 14 Distribution of factor loadings for Factor 2 versus Factor 1

with high HCO_3. It indicates the combined hydrogeochemical processes of seawater intrusion controlling the groundwater chemistry (Lee et al. 2008; Mustapha et al. 2013; Chitsazan et al. 2017).

Factor analysis

Factor analysis is useful to find links among the hydrogeochemical constituents of groundwater samples (Brown, 1998; Kouping et al. 2006). The factors can characterize the principal processes and help the understanding of hydrogeochemical progression (Hussein 2004). Factor loadings were categorized by strong, moderate, and weak corresponding to the loading values of > 0.75, 0.75–0.50, and 0.50–0.30, respectively (Liu et al. 2003; Vetrimurugan et al. 2017). The classification of factor loading values is given in Table 2. It produced two factors with the total variance of 82.9%. The variance and eigenvalue are 66.99% and 11.39 for Factor 1, and 15.94% and 2.71 for
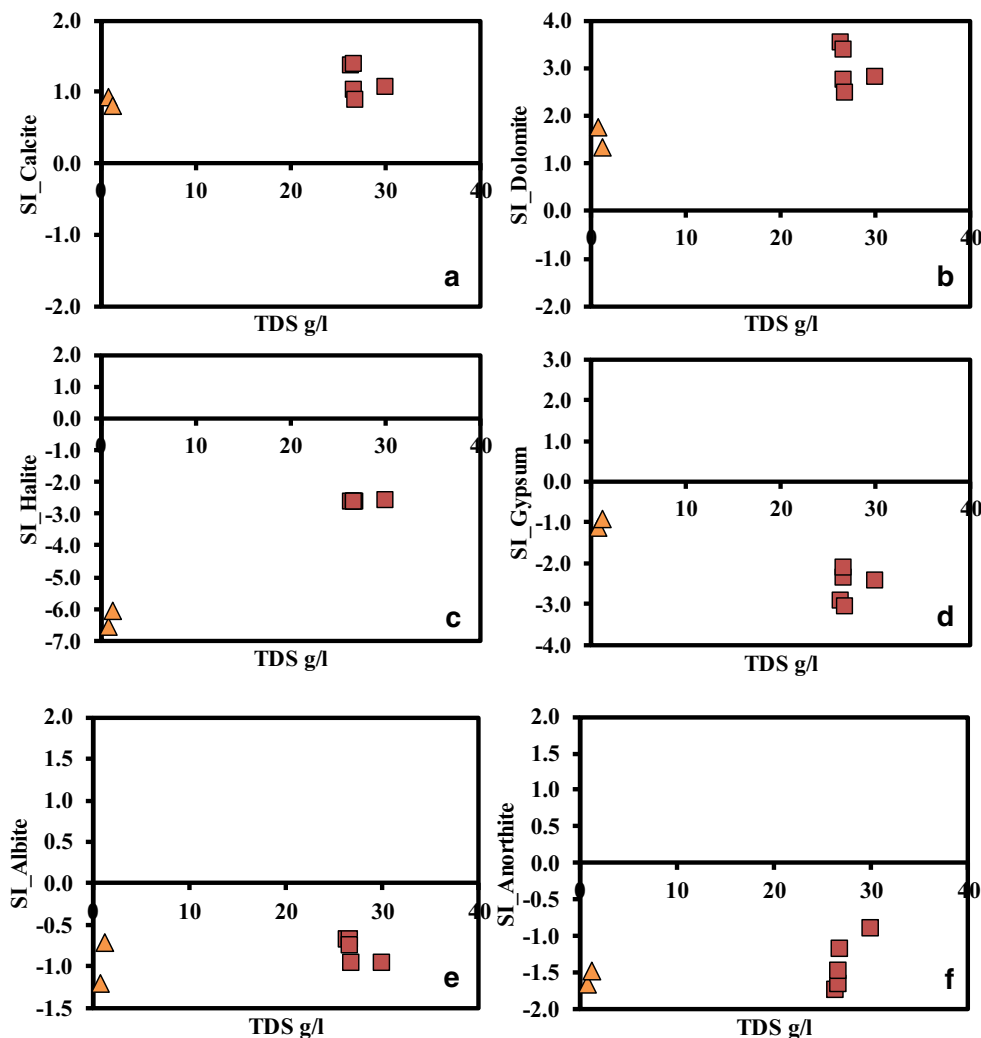
patterns of major cations and anions in the confined aquifer are in the order of Na > Mg > Ca > K, and Cl > HCO_3 > SO_4, respectively. Group 2 includes the NaCl types of groundwater

Fig. 15 Groundwater equilibrium and relationship between saturation states of minerals and the total dissolved solids: **a** SI-calcite, **b** SI-dolomite, **c** SI-halite, and **d** SI-gypsum (e) SI-Albite(f) SI-Anorthite

Factor 2. Variables of EC, TDS, Na, K, Ca, Mg, Cl, HCO$_3$, and As have the strong positive factor loadings for Factor 1, and ORP, SO$_4^{-2}$, and Si had the strong negative factor loadings for Factor 1. DO and Al have the moderate loadings for Factor 2, and pH and Fe have the strong negative loadings for Factor 2. Factor analysis showed that groundwater of the confined aquifer is much influenced by seawater (Factor 1), and that iron and arsenic are dominant heavy metals in groundwater of the confined aquifer (Factor 2).

Figure 14 shows the distribution of factor loadings in two factors. In the first quarter of EC, TDS, Na, Ca, K, Mg, Cl, and HCO$_3$ with the strong positive loadings in Factor 1 form a distinct cluster, and Al and Mn are separated. In the second quarter, ORP and SO4 with the strong negative loadings in Factor 1exist closely and DO with the moderate positive loading in Factor 2 is isolated. The third quarter contains Si of the strong negative factor loading in Factor 1and pH of the strong negative factor loading in Factor 2. The fourth quarter includes As of the strong positive factor loading in Factor 1 and Fe of the strong negative loadings in Factor 2. FA reflects the influence of seawater intrusion (Yaouti et al. 2009). The strong loading of Cl suggests the influences of saline water, industrial effluents, and the long groundwater migration (Kumar and Alappat 2005). HCA and FA supported the factors controlling the groundwater chemistry of this region.

Groundwater modeling

Groundwater equilibrium

The saturation mineral index is calculated by SI = (IAP/Ks), where IAP is the ion activity product and Ks is the solubility product of the mineral (Appelo and Postma 2005). It is very useful to assess the groundwater chemistry and to see if it is well-ordered by equilibrium with solid phases. If SI < 0, SI = 0, and SI > 0, the water is undersaturated, equilibrium, and oversaturated conditions, respectively. The saturation mineral index rate is calculated by precipitation and/or dissolution reactions occurring in groundwater. Figure 15 represents the estimated saturation indices using PHREEQC for calcite, dolomite, gypsum, halite, albite, and anorthite are compared with TDS. Groundwater samples of both confined and unconfined aquifers indicate the oversaturation of calcite and dolomite representing the evaporation and deposition. At the same time, the minerals of gypsum, halite, albite, and anorthite are undersaturated with respect to dissolution (Venkatramanan et al. 2017).

Inverse geochemical modeling

Inverse models for two principal aquifers were formulated like unconfined and confined aquifers. The statistical results of

Table 3

Results of inverse geochemical modeling

Simulation 1 : 10-Models obtained in Unconfined aquifer–Confined aquifer

Initial solution	Well No 4									
Final solution	Well No 5									
Mineral phases	Phase mole transfers Well No 4–Well No 5									
Albite	−1.35E-02	−2.49E-02	−1.35E-02	−1.35E-02	−2.49E-02	−1.35E-02	−2.49E-02	−1.35E-02	−2.49E-02	−1.35E-02
Anorthite	−1.68E-02	−3.14E-02	−1.67E-02	−1.68E-02	−3.14E-02	−1.67E-02	−3.14E-02	−1.67E-02	−3.14E-02	−1.67E-02
Gypsum	−3.79E-03	−3.79E-03	−3.79E-03	–	–	–	−3.79E-03	−3.79E-03	–	–
Halite	4.12E-01	4.23E-01	4.11E-01	4.12E-01	4.23E-01	4.13E-01	4.23E-01	4.11E-01	4.23E-01	4.11E-01
Dolomite	1.81E-02	4.08E-03	2.04E-02	1.81E-02	–	2.04E-02	–	2.04E-02	–	2.04E-02
Calcite	–	–	–	–	–	–	3.58E-02	4.65E-04	3.58E-02	4.65E-04

Simulation 2 7-Models obtained in Unconfined aquifer–Confined aquifer

Initial solution	Well No 3						
Final solution	Well No 2						
Mineral phases	Phase mole transfers Well No 3–Well No 2						
Albite	–	−5.48E-03	–	−8.68E-04	−5.48E-03	1.30E-02	8.68E-04
Anorthite	−1.12E-03	–	−1.12E-03	–	−8.21E-03	−1.58E-02	
Gypsum	−3.27E+02	−3.29E+02	−3.39E+02	−3.27E+02	−3.27E+02	−3.24E+02	−3.27E+02
Halite	3.68E-01	3.73E-01	3.68E-01	3.67E-01	3.73E-01	3.55E-01	3.67E-01
Dolomite	5.46E-02	6.64E-02	5.46E-02	5.28E-02	6.64E-02	2.61E-02	5.28E-02
Calcite	–	–	4.30E-02	–	6.07E-02	–	4.02E-02

Thermodynamic database used: phreeqc.dat values are in moles/kilogram H$_2$O. Positive (entering water) and negative (leaving water) phase mole transfers indicate dissolution and precipitation, respectively. (The dash line represents no mass transfer)

chemical components (Table 1) were used to denote "initial" and "final" water along a groundwater flow path. The saturation indices of common mineral phases clearly showed that groundwater was generally oversaturated with respect to carbonate and silicate minerals, and undersaturated with albite, anorthite, anhydrite, gypsum, and halite. The inverse models were expressed so that primary mineral phases of gypsum, halite, anorthite, and albite could be dissolved until they reach at the saturation state. At this time, calcite and dolomite were set to the precipitated phase (Table 3).

Simulation 1 used the data of Well No.4 of the unconfined aquifer and Well No. 5 of the confined aquifer, and rock-water interaction is supposed to be the principal mechanism for water chemistry. It also used the CaSO$_4$ type for the unconfined aquifer and Na-Cl type for the confined aquifer. Simulation 2 used the data of Well No. 3 of the unconfined aquifer and Well No. 2 of the confined aquifer. The results of two simulations are given in Table 3. Simulation 1 and Simulation 2 describe the evolution from confined to unconfined conditions. Gypsum and halite were selected as precipitated phases, and albite, anorthite, calcite, and dolomite were as dissolved phase. Based on this simulation 1 and simulation 2, 10 models and 7 models were obtained, and mineral phases such as albite, anorthite, gypsum, halite, dolomite, and calcite occurred in this model. Two simulations represented that gypsum was under the precipitated phase, and they were mainly controlled by evaporation and ion exchange processes. The minerals of albite, anorthite, halite, calcite, and dolomite fell under the dissolution phase (Chidambaram et al. 2012).

Inverse geochemical modeling drew the geochemical processes such as the precipitation of gypsum; the dissolution of albite, anorthite, calcite, dolomite, and halite due to the weathering of accessory pyroxene or amphibole minerals; and seawater intrusion (Milnes and Renard, 2004). Exchange of calcium and magnesium in water with sodium in aquifer materials is mainly related with the ion exchange process.

Conclusion

This research work mainly focused on the hydrogeochemical characteristics of confined and unconfined aquifer systems in the deltaic region of the Nakdong River Basin in the Busan Metropolitan City of Korea. Seven groundwater samples were collected from unconfined and confined aquifer systems. Groundwater chemistry of the study area was dominated by the CaSO$_4$ type in the unconfined aquifer and NaCl type in confined aquifer. Chemical constituents of groundwater were strongly influenced by water-rock interaction in the unconfined aquifer. Direct and reverse ion exchanges were two possible processes of water–rock interaction in the study area. Carbonate and silicate weathering were the dominant processes

in the confined aquifer and unconfined aquifer, respectively. The major ion concentrations of groundwater samples were increased by the ion exchange of minerals in the aquifer system.

Groundwater quality analysis was important to identify the processes and mechanism affecting the geochemistry of groundwater. Gibbs plots suggested that groundwater samples of the unconfined aquifer were influenced by the chemical weathering with dissolution of rock forming minerals, and groundwater samples of the confined groundwater were plotted in the evaporation zone. The mineral saturation of dolomite and calcite was oversaturated, while albite, gypsum, and halite were undersaturated. The HCA classify seven groundwater samples into two groups based on the similarity of groundwater characteristics. The first group is exclusively composed of groundwater in the unconfined aquifer, and the second group consists of groundwater in the confined aquifer. Factor analysis also explains two factor loadings. The factor 1 is designated by the strong positive loadings of EC, TDS, Na, K, Ca, Mg, Cl, HCO$_3$, SO$_4$, and Si, and factor 2 exhibits the strong negative loadings of pH and Fe.

The inverse geochemical modeling demonstrated that mineral phases were essential to derive the variances in groundwater chemistry along the flow path in the area. This modeling proposed that carbonate dissolution and ion exchange processes were the leading geochemical processes in this region. It drew the geochemical processes controlled by the precipitation of gypsum; the dissolution of calcite, dolomite, and halite; and the weathering of albite and anorthite.

This work also emphasizes the importance of the combined studies of hydrogeochemical and multivariate statistical methods in studying the sources and processes of groundwater quality deterioration. Further studies are necessary to determine the degree of groundwater contamination using other techniques such as contaminant transport modeling and isotopic analysis, and to manage groundwater effectively in the Nakdong deltaic region.

References

Adams S, Titus R, Pietersen K, Tredoux G, Harris C (2001) Hydrochemical characteristics of aquifers near Sutherland in the Western Karoo, South Africa. J Hydrol 241:91–103

APHA (American Public Health Association) (1995) Standard methods for the examination of water and wastewater, 19th edn. American Public Health Association, Washington, DC, p 1467

Appelo CAJ, Postma D (2005) Geochemistry, groundwater and pollution, 2nd edn. Balkema, Amsterdam, p 321

Ashley RP, Lloyd JW (1978) An example of the use of factor analysis and cluster analysis in groundwater chemistry interpretation. J Hydrol 39:355–364

Belkhiri L, Boudoukha A, Mouni L, Baouz T (2010) Application of multivariate statistical methods and inverse geochemical modeling for characterization of groundwater—a case study: Ain Azel plain (Algeria) Geoderma 159 :390–398

Bose P, Sharma A (2002) Role of iron in controlling speciation and mobilization of arsenic in subsurface environment. Water Res 36(19):4916–4926

Brindha K, Pavelic P, Sotoukee T, Somphasith D, Elango L (2017) Geochemical characteristics and groundwater quality in the Vientiane Plain, Laos. Expo Health 9:89

Brown KG (1998) Assessing risk of inorganic arsenic in drinking water in the United States. Human Ecol Risk Assess 4(5):1061–1070

Chidambaram S, Anandhan P, Prasanna MV, Ramanathan AL, Srinivasamoorthy K, Senthil Kumar G (2012) Hydrogeochemical modelling for groundwater in Neyveli Aquifer, Tamil Nadu, India, using PHREEQC: a case study. Nat Resour Res 21:311–324

Chitsazan M, Aghazadeh N, Mirzaee Y, Golestan Y, Mosavi S (2017) Hydrochemical characteristics and quality assessment of urban groundwater in Urmia City. NW Iran Water Sci Technol Water Supply. https://doi.org/10.2166/ws.2017.039

Cho A, Cheong D, Kim JC, Shin S, Park YH, Katsuki K (2017) Delta formation in the Nakdong River, Korea, during the Holocene as inferred from the diatom assemblage. J Coast Res 33:67–77

Chung SY, Venkatramanan S, Park N, Rajesh R, Ramkumar T, Kim BW (2014) An assessment of selected hydrochemical parameter trend of the Nakdong River water in South Korea, using time series analyses and PCA, Environ Monit Assess (2015) 187:4192

Chung SY, Venkatramanan S, Park N, Ramkumar T, Sujitha SB, Jonathan MP (2016) Evaluation of physico-chemical parameters in water and total heavy metals in sediments at Nakdong River Basin, Korea. Environ Earth Sci 75(1):50

Chung SY, Rajesh R, Venkatramanan S (2019) Evaluation of heavy-metal contamination in groundwater using hydrogeochemical and multivariate statistical analyses. GIS and geostatistical techniques for groundwater science. https://doi.org/10.1016/B978-0-12-815413-7.00024-9. 331–346

Daniele L, Vallejo Á, Corbella M, Molina L, Pulido-Bosch A (2013) Hydrogeochemistry and geochemical simulations to assess water-rock interactions in complex carbonate aquifers: the case of Aguadulce (SE Spain). Appl Geochem 29:43–54

Datta PS, Tyagi SK (1996) Major ion chemistry of groundwater in Delhi area: chemical weathering processes and groundwater regime. Geol Soc India 47:179–188

de Caritat P, Bastrakov EN, Jaireth S, English PM, Clarke JDA, Mernagh TP, Wygralak AS, Dulfer HE, Trafford J (2019) Groundwater geochemistry, hydrogeology and potash mineral potential of the Lake Woods region, Northern Territory, Australia. Aust J Earth Sci 66(3):411–430

Helena B, Pardo R, Vega M, Barrado E, Fernandez JM, Fernandez L (2000) Temporal evolution of groundwater composition in an alluvial (Pisuerga river, Spain) by principal component analysis. Water Res 34:807–816

Hussein MT (2004) Hydrochemical evaluation of groundwater in the Blue Nile Basin, eastern Sudan, using conventional and multivariate techniques. Hydrogeol J 12:144–158

Iticescu C, Georgescu LP, Topa CM (2013) Assessing the Danube water quality index in the city of Galati, Romania. Carpathian Journal of Earth and Environmental Sciences 8:155–164

Jankowski J, Acworth RI (1997) Impact of debris-flow deposits on hydrogeochemical process and the development of dry land salinity in the Yass River catchment, New South Wales, Australia. Hydrogeol J 5(4):71–88

Kouping C, Jiao JJ, Huang J, Huang R (2006) Multivariate statistical evaluation of trace elements in groundwater in a coastal area in Shenzhen, China. Environ Pollut 147:771–780

Kumar D, Alappat BJ (2005) Analysis of leachate pollution index and formulation of sub-leachate pollution indices. Waste Manag Res 23(3):230–239

Kumar M, Kumari K, Singh UK, Ramanathan A (2009) Hydrogeochemical processes in the groundwater environment of Muktsar, Punjab: conventional graphical and multivariate statistical approach. Environ Geol 57(4):873–884

Lee YJ, Choi JM, Oertel GF (2008) Postglacial sea-level change of the Korean Southern Sea shelf. J Coast Res 24(4A):118–132

Li P (2016) Groundwater quality in Western China: challenges and paths forward for groundwater quality research in Western China. Expo Health 8(3):305–310

Li P-Y, Qian H, Wu J-H, Ding J (2010) Geochemical modeling of groundwater in southern plain area of Pengyang County, Ningxia, China. Water Sci and Engineering 3(3):282–291

Liu CW, Lin KH, Kuo YM (2003) Application of factor analysis in the assessment of groundwater quality in a blackfoot disease area in Taiwan. Sci Total Environ 313(1–3):77–89

Maya AL, Loucks MD (1995) Solute and isotopic geochemistry and groundwater flow in the Central Wasatch Range. Utah J Hydrol 172:31–59

Mayback M (1987) Global chemical weathering of surficial rocks estimated from river dissolved loads. Am J Sci 287:401–428

McLaughlin D, Townley LLR (1996) A reassessment of the groundwater inverse problem. Water Resour Res 32(5):1131–1161

Meng SX, Maynard JB (2001) Use of multivariate analysis to formulate conceptual models of geochemical behavior: water chemical data from the Botucata Aquifer in Sao Paulo state, Brazil. J Hydrol 250:78–97

Mohamed MM, Elmahdy SI (2015) Natural and anthropogenic factors affecting groundwater quality in the eastern region of the United Arab Emirates. Arab J Geosci 8:7409

Mustapha A, Aris AZ, Juahir H, Ramli MF, Kura NU (2013) River water quality assessment using environmentric techniques: case study of Jakara River basin. Environ Sci Pollut Res 20:5630–5644

Parkhurst DL, Appelo CAJ (1999) User's guide to PHREEQC (version 2)—a computer program for speciation, batch-reaction, one-dimensional transport, and inverse geochemical calculations: geological survey. Denver, Colorado, p 312

Paul R, Brindha K, Gowrisankar G, Tan ML, Mahesh Kumar S, Tan ML (2019) Identification of hydrogeochemical processes controlling groundwater quality in Tripura, Northeast India using evaluation indices, GIS, and multivariate statistical methods. Environ Earth Sci 78:470

Pereira HG, Renca S, Sataiva J (2003) A case study on geochemical anomaly identification through principal component analysis supplementary projection. Appl Geochem 18:37–44

Prasanna MV, Chidambaram S, Thilagavathi R, Thivya C, Venkatramanan S, Murali Krishnan N (2019) A statistical approach to identify the temporal and spatial variations in the geochemical process of a coastal aquifer, South East Coast of India. GIS and Geostatistical Techniques for Groundwater, p.223–235, https://doi.org/10.1016/B978-0-12-815413-7.00016-X

Rajesh R, Brindha K, Murugan R, Elango L (2012) Influence of hydrogeochemical processes on temporal changes in groundwater quality in a part of Nalgonda district, Andhra Pradesh, India. Environ Earth Sci 65:1203–1213

Razack M, Dazy J (1990) Hydrochemical characterization of groundwater mixing in sedimentary and metamorphic reservoirs with combined use of Piper's principle and factor analysis. J Hydrol 114(3–4):371–393

Srivastava SK, Ramanathan AL (2008) Geochemical assessment of groundwater quality in vicinity of Bhalswa Landfill, Delhi, India. Using Graph Multivar Stat Methods Environ Geol 53:1509–1528

Stark JR, Hanson PE, Goldstein RM, Fallon JD, Fong AL, Kroening SE, Andrews WJ (2000) Water quality in the Upper Mississippi River Basin, Minnesota, Wisconsin, South Dakota. United States Geological Survey, Circular 1211:1995–1998

StatSoft (2015) STATISTICA ver 9. http://www.statsoft.com

Sun NZ (1994) Inverse problems in groundwater modeling. Publishers, Kluwer Academic

Thilagavathi R, Chidambaram S, Thivya C, Tirumalesh K, Venkatramanan S, Pethaperumal S, Prasanna MV, Ganesh N (2019) Influence of variations in rainfall pattern on the hydrogeochemistry of coastal groundwater—an outcome of periodic observation. Environ Sci Pollut Res. https://doi.org/10.1007/s11356-019-05962-w

Venkatramanan S, Chung SY, Lee SY, Park N (2014) Assessment of river water quality via environmentric multivariate statistical tools and water quality index: a case study of Nakdong River Basin, Korea. Carpathian J Earth Environ Sci 9(2):125–132

Venkatramanan S, Chung SY, Selvam S, Son JH, Kim YJ (2017) Interrelationship between geochemical elements of sediment and groundwater at Samrak Park Delta of Nakdong River Basin in Korea: multivariate statistical analyses and artificial neural network approaches. Environ Earth Sci 76:456

Vetrimurugan E, Brindha K, Sithole B, Elango L (2017) Spatial interpolation methods and geostatistics for mapping groundwater contamination in a coastal area. Environ Sci Pollut Res 24:11601. https://doi.org/10.1007/s11356-017-8681-6

Walker BR, Jolly LD, Cook PG (1991) A new chloride leaching approach to the estimation of diffuse recharge following a change in land use. J Hydrol 128:49–67

Werner A, Bakker M, Post VEA, Vandenbohede A, Lu C, Ataie-Ashtiani B, Simmons CT, Barry DA (2013) Seawater intrusion processes, investigation and management: recent advances and future challenges. Adv. Water Resour 51:3–26

Wu J, Sun Z (2016) Evaluation of shallow groundwater contamination and associated human health risk in an alluvial plain impacted by agricultural and industrial activities, mid-west China. Expo Health 8(3):311–329

Wu J, Li P, Qian H, Duan Z, Zhang X (2014) Using correlation and multivariate statistical analysis to identify hydrogeochemical processes affecting the major ion chemistry of waters: case study in Laoheba phosphorite mine in Sichuan, China. Arab J Geosci 7(10):3973–3982

Yaouti FE, Mandour AE, Khattach D, Benavente J, Kaufmann O (2009) Salinization processes in the unconfined aquifer of Bou-Areg (NE Morocco): a geostatistical, geochemical, and tomographic study. Appl Geochem 24:16–31

Yoo DG, Kim SP, Changa TS, Konga GS, Kanga NK, Kwonb YK, Namc SL, Park SC (2014a) Late Quaternary inner shelf deposits in response to late Pleistocene–Holocene Sea level changes: Nakdong River. SE Korea, Quaternary Inter 344:156–169

Yoo DG, Kim SP, Lee CW, Chang TS, Kang NK, Lee GS (2014b) Late Quaternary transgressive deposits in a low-gradient environmental setting: Korea Strait shelf, SE Korea, Quaternary Inter, 344:143–155

Zaki SR, Redwan M, Masoud AM, Ahmed A, Moneim A (2019) Chemical characteristics and assessment of groundwater quality in Halayieb area, southeastern part of the Eastern Desert, Egypt. Geosci J 1:149–164

Zhu C, Anderson G (2002) Environmental applications of geochemical modeling. Cambridge University Press, Cambridge, p 284